# CHAPTER 5

## Assessing the Risk of a Collapse of the Atlantic Thermohaline Circulation

Michael E. Schlesinger[1], Jianjun Yin[2], Gary Yohe[3], Natalia G. Andronova[4], Sergey Malyshev[5] and Bin Li [1]
[1]*Climate Research Group, Department of Atmospheric Sciences, University of Illinois at Urbana-Champaign*
[2]*Program in Atmospheric & Oceanic Sciences, Princeton University*
[3]*Department of Economics, Wesleyan University*
[4]*Department of Atmospheric, Oceanic and Space Sciences, University of Michigan*
[5]*Department of Ecology and Evolutionary Biology, Princeton University*

ABSTRACT: In this paper we summarize work performed by the Climate Research Group within the Department of Atmospheric Sciences at the University of Illinois at Urbana-Champaign (UIUC) and colleagues on simulating and understanding the Atlantic thermohaline circulation (ATHC). We have used our uncoupled ocean general circulation model (OGCM) and our coupled atmosphere-ocean general circulation model (AOGCM) to simulate the present-day ATHC and how it would behave in response to the addition of freshwater to the North Atlantic Ocean. We have found that the ATHC shuts down 'irreversibly' in the uncoupled OGCM but 'reversibly' in the coupled AOGCM. This different behavior of the ATHC results from different feedback processes operating in the uncoupled OGCM and AOGCM. We have represented this wide range of behaviour of the ATHC with an extended, but somewhat simplified, version of the original model that gave rise to the concern about the ATHC shutdown. We have used this simple model of the ATHC together with the DICE-99 integrated assessment model to estimate the likelihood of an ATHC shutdown between now and 2205, both without and with the policy intervention of a carbon tax on fossil fuels. For specific subjective distributions of three critical variables in the simple model, we find that there is a greater than 50% likelihood of an ATHC collapse, absent any climate policy. This likelihood can be reduced by the policy intervention, but it still exceeds 25% even with maximal policy intervention. It would therefore seem that the risk of an ATHC collapse is unacceptably large and that measures over and above the policy intervention of a carbon tax should be given serious consideration.

### 5.1 Introduction

The Atlantic thermohaline circulation (ATHC) is driven by temperature (thermo) and salt (haline) forcing over the ocean surface (Stommel, 1961). The ATHC currently transports poleward about 1 petawatt ($10^{15}$ W) of heat, that is, a million billion Watts. Since human civilization currently uses 10 terawatts of energy ($10^{13}$ W), the heat transported by the ATHC could run 100 Earth civilizations. Conversely, 1% of the heat transported by the ATHC could supply all of humanity's current energy use. As a result of this enormous northward heat transport, Europe is up to 8°C warmer than other longitudes at its latitude, with the largest effect in winter. It is this comparatively mild European climate, as well as the inter-related climates elsewhere, that has given concern about the possible effect of a collapse of the ATHC, in terms of political and economic instability (Gagosian, 2003, Schwartz and Randall, 2003) and the onset of an ice age (Emmerich, 2004). Public concern has also been expressed in the novel 'Forty Signs of Rain' (Robinson, 2004) – the first book in a trilogy about a human-induced 'stall' of the ATHC – with an opposing view expressed in the novel 'State of Fear' (Crichton, 2004).

Why would the ATHC collapse? There are two threads of evidence that suggest this possibility. One is based on modeling and the other is drawn from paleoclimate evidence. The first model of the ATHC was developed by Henry Stommel (1961), which is the simplest possible model to study the dynamical behavior of the ATHC. In this very simple model, heat and salt are transported from an equatorial box to a polar box, with each box taken to have its own temperature and salinity. The direction of the net transport is the same regardless of whether the circulation is clockwise (viewed from Europe toward North America) as for the present-day ATHC configuration or counterclockwise – a reversed ATHC. Many years later Barry Saltzman (2002) simplified the model to consider only salt transport. He took the temperature difference between the boxes as being constant and extended the model to include salt transport by the non-THC motions in the ocean – the wind-driven gyre circulation and eddies akin to weather disturbances in the atmosphere.

As freshwater is added to the polar box in the Stommel-Saltzman (S-S) model the ATHC intensity weakens because the density of the polar box decreases, leading to a reduction in the density differential between the equatorial box and the polar box. As increasing amounts of freshwater are added, the intensity continues to decrease, but only to a point. At this threshold or bifurcation point, this continuous behavior ceases and is replaced by a nonlinear abrupt change to a counterclockwise reversed ATHC (RTHC). Further addition of freshwater enhances

the intensity of this RTHC. More importantly, a reduction of the freshwater addition does not cause the circulation to return to the bifurcation point from which it came. Rather, it weakens the RTHC. Eventually, if the freshwater addition is reduced sufficiently, another bifurcation point is reached such that the ATHC abruptly restarts. This irreversible behavior of the ATHC in the S-S model results in hysteresis – a change in the system from one stable equilibrium to another and then back along a different path.

Why should there be an additional freshwater addition to the North Atlantic Ocean? The surface air temperature of central Greenland has been reconstructed as a function of time from about 15,000 years ago to the present based on the isotopic composition of an ice core that was drilled in the Greenland ice sheet (Alley et al., 1993, Taylor et al., 1997, Alley, 2000). The reconstruction shows a rise in surface air temperature at the end of the last Ice Age nearly 15,000 years ago followed by a return to Ice Age conditions thereafter for about 2000 years. During this episode, an Arctic plant called Dryas *Octopetala* arrived in Europe, hence the appellation Younger Dryas. Additional evidence that the Younger Dryas was global in extent has been provided by terrestrial pollen records, glacial-geological data, marine sediments, and corals (e.g. Chinzei et al., 1987, Atkinson et al., 1987, Alley, 2000, McManus, 2004). This evidence of abrupt cooling in the North Atlantic and Europe has been taken as being due to a slowdown or collapse of the ATHC. This ATHC slowdown/shutdown appears to have occurred as the meltwater stored in Lake Agassiz from the retreating Laurentide ice sheet on North America, which had previously flowed to the Gulf of Mexico via the Mississippi River, instead flowed out either the St. Lawrence waterway to the North Atlantic Ocean (Johnson and McClue, 1976, Rooth, 1982, Broecker, 1985, Broecker et al., 1988, Broecker et al., 1989, Broecker, 1997, Alley, 1998, Teller et al., 2002, Broecker, 2003, Nesje et al., 2004, McManus et al., 2004) or to the Arctic Ocean via the Mackenzie River and then to the North Atlantic Ocean (Tarasov and Peltier, 2005), thereby freshening it sufficiently to slow down or halt the ATHC.

So the ATHC has apparently slowed or shut down in the past. Might it do so in the future as a result of global warming? The ATHC intensity simulated by 9 AOGCMs for a scenario of future IS92a greenhouse gas emissions (IS92a, Leggett et al., 1992) slows down for all models but one (Cubasch et al., 2001, Figure 9.21). As the world warms, both precipitation (P) and evaporation (E) increase over the North Atlantic, but the difference (P − E) also increases there. Freshwater is thereby added to the ocean. Both the surface ocean freshening and warming reduces the density of the surface water and thus its ability to sink (Manabe and Stouffer, 1994).

In the AOGCM simulations of a greenhouse-gas (GHG)-induced slowdown or shutdown of the ATHC, the resulting climate change is due to both the increased concentrations of GHGs and to the ATHC change. However, the magnitude of GHG-induced climate change required to slowdown or shutdown the ATHC is highly uncertain. Thus, it is desirable to separate the ATHC-induced climate change from the GHG-induced climate change so that they can subsequently be combined to address a series of critical questions. Suppose the ATHC begins to slowdown for a change of global-mean surface air temperature of x°C due to increased concentrations of GHGs: (1) What would the resulting climate changes look like? (2) What would the impacts of those changes look like? and (3) What near-term policies are robust against the uncertainty of an ATHC slowdown/shutdown (Lempert and Schlesinger, 2000)?

We began a program of research in 1999 that would allow us to answer the first of these questions by simulating the slowdown and shutdown of the ATHC using our AOGCM. We performed our ATHC-shutdown simulations first with our uncoupled ocean GCM (OGCM) and then with it coupled to our atmospheric GCM. Like all other simple models (Rahmstorf, 1995, Ganopolski and Rahmstorf, 2001, Schmittner and Weaver, 2001, Titz et al., 2002, Prange et al., 2002, Schmittner et al., 2002, Rahmstorf, 1995) beginning with that of Stommel (1961), the OGCM simulated an irreversible ATHC shutdown. By way of contrast, though, the AOGCM simulated a reversible ATHC shutdown, as found by all AOGCMs (Schiller et al., 1997, Manabe and Stouffer, 1999, Rind et al., 2001, Vellinga et al., 2002) other than by Manabe and Stouffer (1988). Below we describe this finding, comparing for the first time a single uncoupled and coupled OGCM, and note that the S-S model can reproduce not only the irreversible ATHC shutdown, but also the reversible ATHC shutdown. We shall also discuss some of the climate changes induced by the ATHC collapse simulated by our AOGCM. Subsequently, we will use the S-S model with wide-ranging behavior to examine how to reduce the risk of an ATHC collapse.

## 5.2 Simulations of the ATHC Shutdown with the UIUC OGCM and AOGCM

The zonally integrated meridional circulation in the Atlantic Ocean simulated by the UIUC coupled atmosphere/ocean general circulation model (AOGCM) in its control simulation for present-day conditions is shown in Figure 5.1. The ocean currents simulated by the AOGCM in the upper (0–1000 m) and deep (1000–3000 m) Atlantic Ocean are shown in Figure 5.2. A longitude-depth cross-section of currents at 30°N and 50°N is shown in Figure 5.3.

Below we describe the freshwater perturbation experiments that we have performed with our OGCM and AOGCM, discuss the climate changes induced by a collapse of the ATHC, and describe how the S-S model is capable of simulating a range of ATHC shutdown behavior, from an irreversible collapse to a reversible one.

### 5.2.1 *Freshwater Perturbation Experiments*

The freshwater perturbation experiments with the uncoupled OGCM were performed by very slowly increasing and

then decreasing the external freshwater addition to the North Atlantic between 50°∼70°N latitudes (Rahmstorf, 1995). The freshwater perturbation changes at a rate of 0.2 Sv (Sv = $10^6 m^3$/sec) per 1000 years. Although the setup of the experiment is a transient run, the ATHC is always in quasi-equilibrium with the external freshwater forcing due to the extremely slow change of the freshwater perturbation flux. To facilitate comparison with the AOGCM simulations, several steady-state runs with fixed freshwater perturbations were also carried out using the uncoupled OGCM.

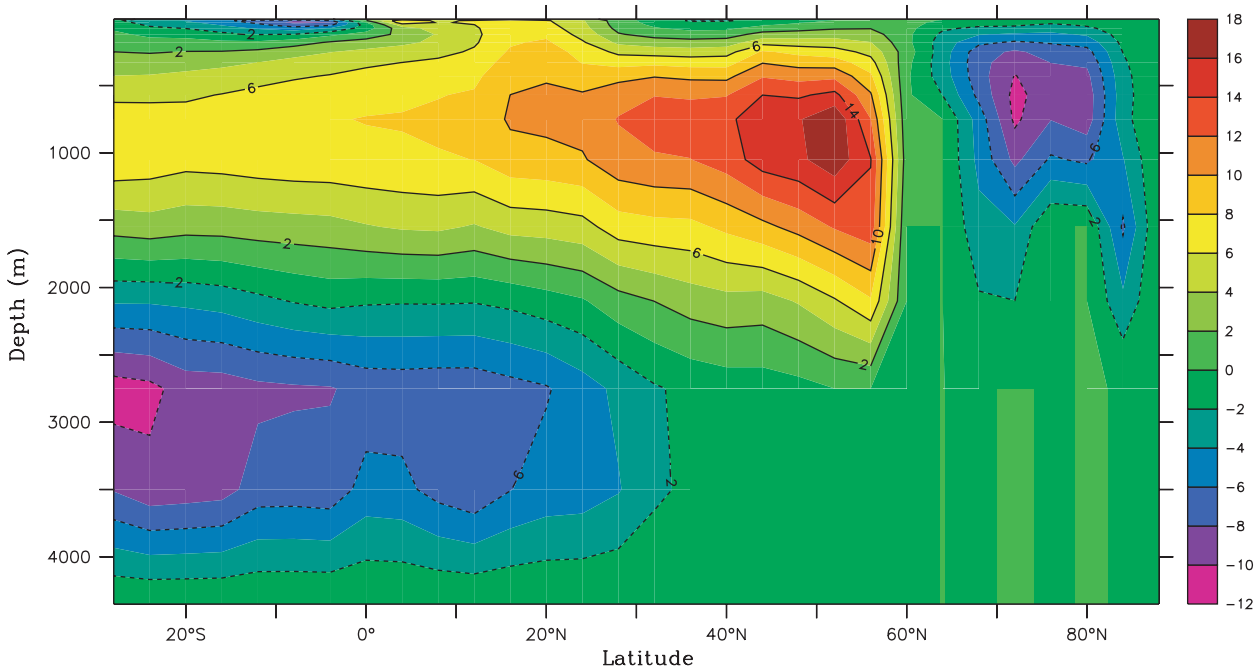


**Figure 5.1** Zonally integrated meridional streamfunction simulated by the UIUC AOGCM.

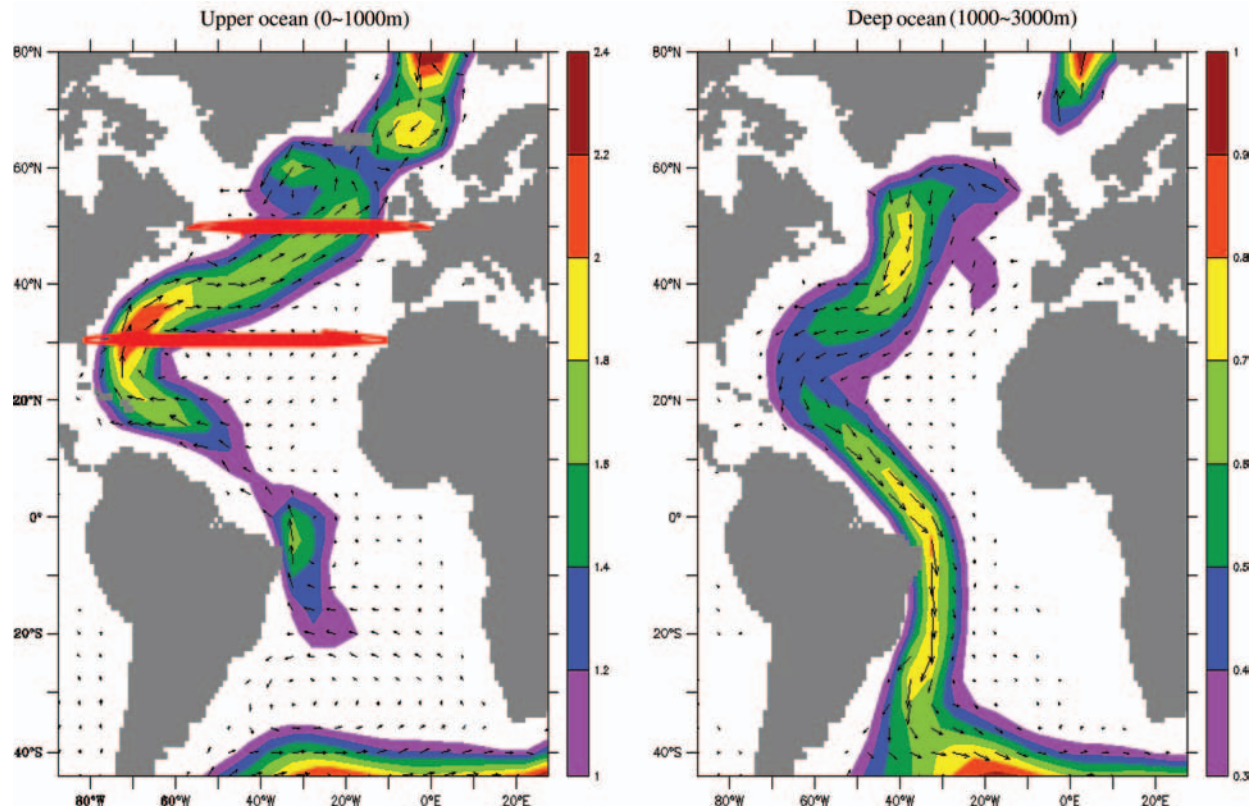


**Figure 5.2** Plan view of the ocean currents (cm/s) simulated by the UIUC AOGCM. The vectors show the current direction and the contours indicate the velocity. The arrows in the left panel show the locations of the longitude-depth cross-sections in Fig. 5.3.

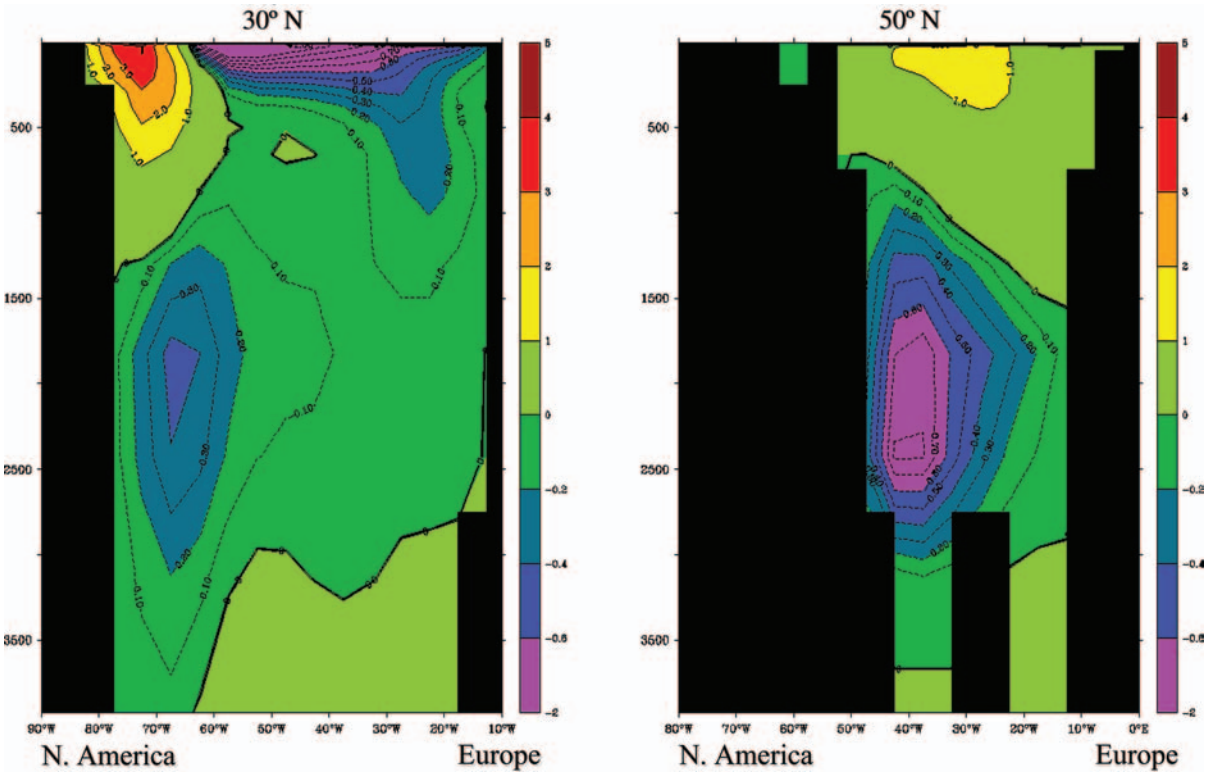


**Figure 5.3** Longitude-depth cross-section at 30°N and 50°N of meridional current (cm/s) simulated by the AOGCM.

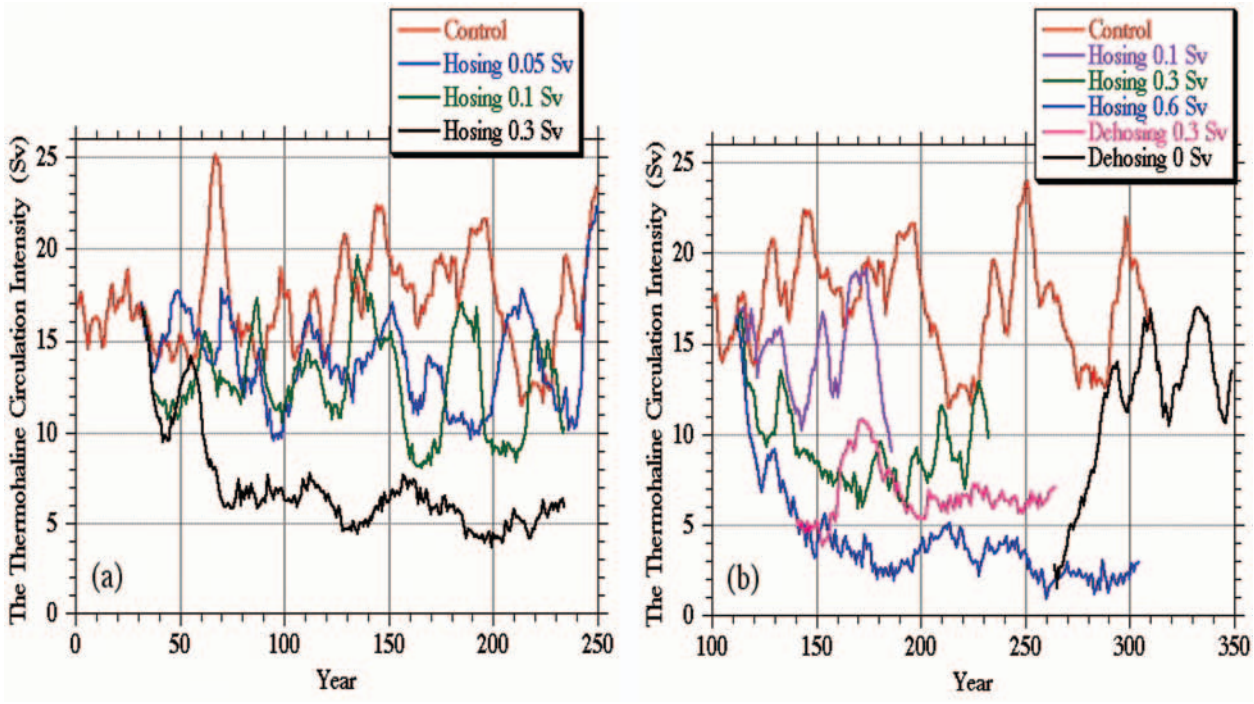


**Figure 5.4** Evolution of the meridional mass streamfunction in the AOGCM hosing and dehosing simulations. (a) The experiments starting from the 30th year of the control; (b) the experiments starting from the 110th year of the control.

The set of AOGCM simulations was performed for fixed freshwater addition ('hosing') and removal ('dehosing') rates over the same latitude band in the North Atlantic as for the OGCM-only simulations (Figure 5.4). Two groups of freshwater perturbation experiments were carried out to test the response of the ATHC. The first group included three 'hosing' experiments starting from the 30th year of the control run. Perturbation freshwater

fluxes of 0.05, 0.1 and 0.3 Sv were uniformly input into the perturbation region in separate experiments. The 110th year of the control run was chosen as the initial condition for the second group. This group consisted of three 'hosing' experiments (0.1, 0.3 and 0.6 Sv) and two 'dehosing' experiments. The two 'dehosing' experiments started from the shutdown state of the ATHC induced by the 0.6 Sv freshwater addition, and included a moderate reduction of the perturbation flux from 0.6 to 0.3 Sv and the total elimination of the 0.6 Sv freshwater addition.

The strength of the ATHC simulated by the uncoupled OGCM with boundary conditions of prescribed heat and freshwater fluxes from the atmosphere has a pronounced hysteresis loop in which the ATHC, after shutdown, can be restarted only after the freshwater addition is eliminated and changed into a freshwater extraction (Figure 5.5a). Three equilibria of the ATHC coexist under the present-day freshwater forcing. Points a and e correspond to two active ATHC modes, while point c is an inactive ATHC mode. The different intensity between points a and e is caused by the switch-on (point e) and switch-off (point a) of deep convection in the Labrador Sea. Points b and d are thresholds along the hysteresis curves. Beyond these critical points, the ATHC undergoes a rapid transition between the active and inactive modes. All of these features indicate a remarkable nonlinearity of the ATHC in the ocean-only model, which results from the domination by the positive feedbacks in the ATHC system. This irreversibility of the ATHC shutdown, if true, would warrant the use of precaution in formulating climate policy.

In contrast, the strength of the ATHC simulated by the AOGCM does not have a hysteresis loop when the freshwater added to the North Atlantic is increased until shutdown occurs and is then reduced (Figure 5.5b). Instead, once the freshwater addition is reduced from its shutdown value, the ATHC restarts. Furthermore, the relation between the ATHC intensity and the change in freshwater addition is roughly linear throughout the entire range of freshwater addition. Moreover, the freshwater addition required to shut down the ATHC is much larger for the AOGCM than for the uncoupled OGCM.

Why does the ATHC behave differently in the uncoupled OGCM and the AOGCM? Yin (2004) and Yin et al. (2005) investigated this question and found different feedback processes operating in the uncoupled OGCM and AOGCM. After the shutdown of the ATHC, a reversed cell develops in the upper South Atlantic in the uncoupled OGCM. This ATHC reversal cannot occur in the AOGCM simulation. The reversed cell transports a large amount of salt out of the Atlantic basin and facilitates the decrease of the basin-averaged salinity in the Atlantic, thereby stabilizing the 'off' mode of the ATHC in the uncoupled OGCM. In contrast, the salinity increases in the Caribbean in the AOGCM simulation of the ATHC shutdown because the intertropical convergence zone shifts from the Northern Hemisphere into the Southern Hemisphere, thereby decreasing the precipitation over the

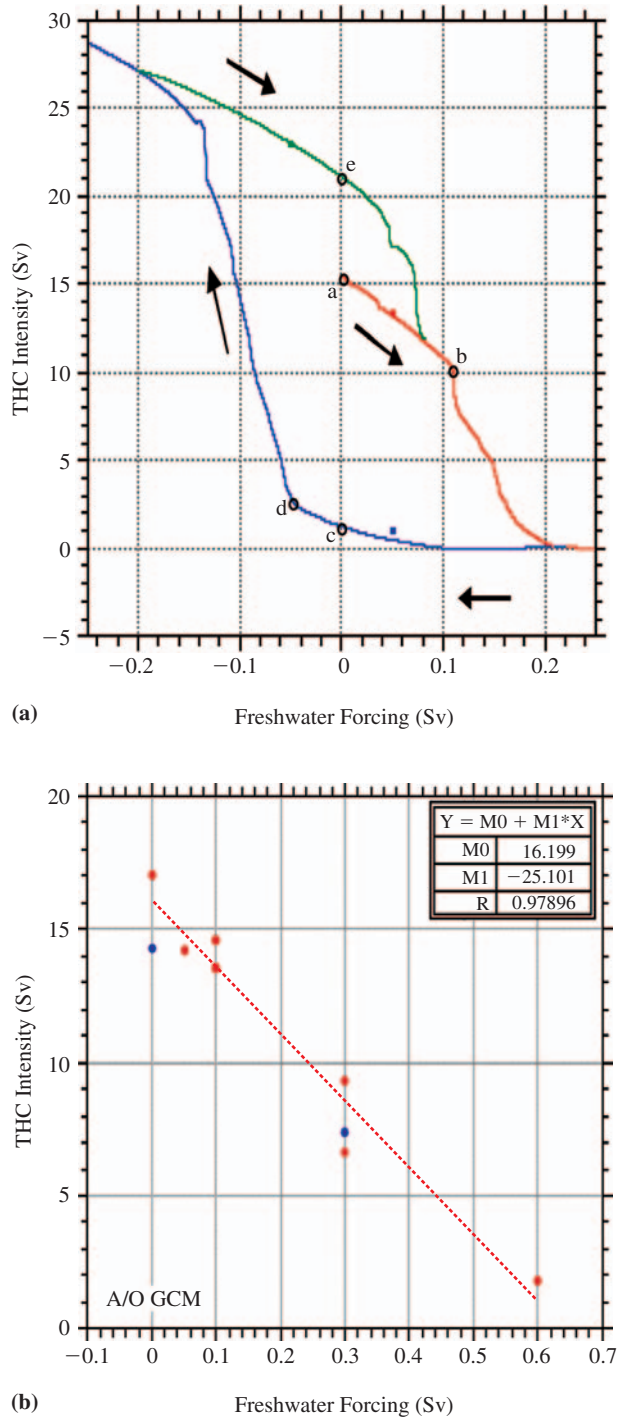


**Figure 5.5** The stability diagrams of the ATHC established by the uncoupled OGCM and the coupled AOGCM. (a) The OGCM with prescribed surface heat and salinity fluxes; (b) The AOGCM (50-year mean). Red, blue and green colors represent the increase in freshwater addition, the subsequent decrease in freshwater addition after the ATHC is shut down, and the following increase in freshwater addition. The origin of the x axis represents the 'present-day' freshwater flux. The rectangles indicate the equilibrium runs with the uncoupled OGCM. The red points in (b) with the same freshwater forcing come from the two simulation groups. The red dashed line is the linear fit based on the red points.

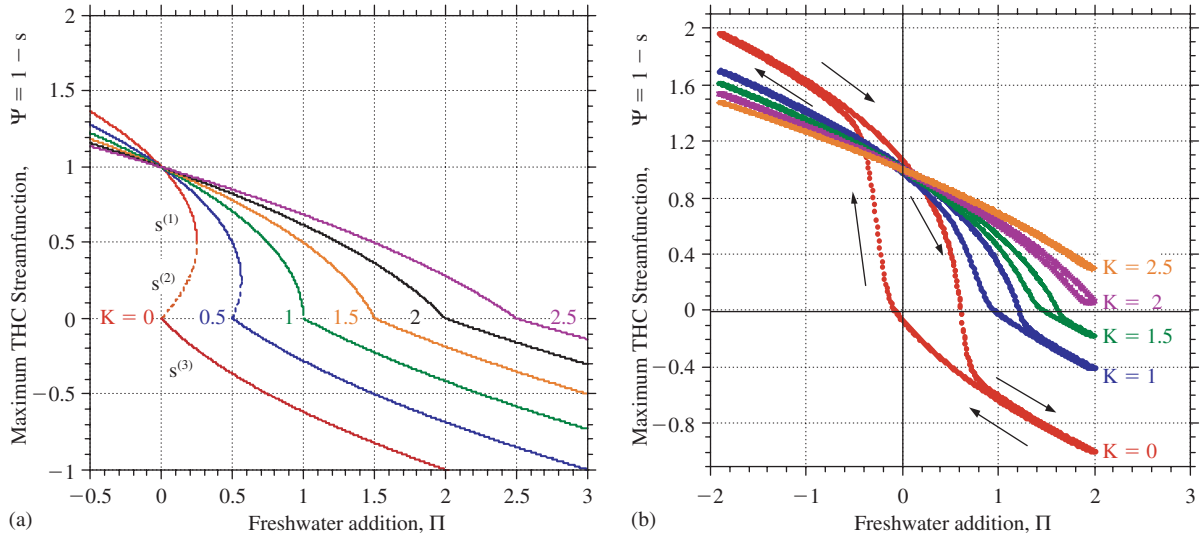


**Figure 5.6** Maximum ATHC streamfunction Ψ versus freshwater addition Π in the S-S model for K from 0 to 2.5: (a) equilibrium and (b) hosing-dehosing simulation.

Caribbean. The resulting more-dense salty water is then transported poleward by the gyre circulation in the North Atlantic. This acts as a negative feedback on the ATHC shutdown which works both to make it more difficult to shut down the ATHC – a larger freshwater addition is required than in the uncoupled OGCM – and to help restart the ATHC when the freshwater, which has been added to shut down the ATHC, is reduced. This negative feedback cannot exist in the uncoupled OGCM simulations because of the need therein to prescribe boundary conditions in the atmosphere.

### 5.2.2 *Climate Changes Induced by an ATHC Shutdown*

In the 0.6 Sv hosing experiment simulated by the AOGCM, the clockwise meridional circulation of the control run is eliminated. A clockwise circulation near 15°N latitude at the surface remains due to the wind-driven upwelling and downwelling. The ocean currents in the upper (0–1000 m) and deep (1000–3000 m) Atlantic Ocean simulated by the AOGCM of the control run both collapse in the 0.6 Sv hosing simulation. The counter-clockwise Antarctic Bottom Water (AABW) circulation centered near 3000 m that is caused by water sinking off the West Antarctic coast is barely influenced by the shutdown of the ATHC in the North Atlantic.

The January and July surface air temperatures resulting from the ATHC shutdown in the 0.6 Sv simulation are lower over the U.S. midwest, Greenland, the North Atlantic Ocean and Europe, with larger cooling in winter than in summer. Interestingly, strong warming occurs over Alaska and the Palmer Peninsula in Northern Hemisphere and Southern Hemisphere winter, respectively. If such a simulated warming were to occur, it would likely harm the Alaskan permafrost and the West Antarctic ice sheet that is grounded on the ocean floor.

### 5.2.3 *Simulation of the ATHC Shutdown by a Simple Model*

As noted in the Introduction, it was the simple two-box model proposed by Stommel (1961) that raised the first alert that the ATHC could collapse irreversibly if sufficient freshwater were added there to reach its threshold bifurcation point. Here we describe how this model, as generalized by Saltzman (2002), can simulate not only an irreversible ATHC collapse, as obtained by all simple models, but also the reversible ATHC shutdown described above which is obtained by most AOGCMs (Yin, 2004). The calibration of the S-S model is described in the Appendix.

The ATHC simulated by the S-S model exhibits sharply-different behavior for different values of the ratio of the transport coefficient K for the gyre circulation and eddies to that for the ATHC. For K = 0 (the case examined by Stommel (1961)) there is an unstable equilibrium circulation connecting two stable equilibrium circulations; one displays sinking in high latitudes and upwelling in low latitudes while the other moves in the opposite direction (Figure 5.6a). As K increases from zero to unity, the range examined by Saltzman (2002), the region of the unstable equilibrium shrinks. Larger values of freshwater addition are required to weaken the ATHC intensity to any particular value. When K takes the value of unity, the unstable equilibrium circulation disappears, and the two stable equilibrium circulations merge. In this case the flow between the two boxes is the combination of wind-driven flow and ATHC flow. The contribution of the wind-driven flow to the poleward salinity transport is significant. As K is increased above unity – a case examined by Yin (2004) and Yin et al. (2005) – still larger values of freshwater addition are required to weaken the ATHC to any particular intensity, and the discontinuity in slope between the two stable circulations decreases. The curve gradually

approaches a straight line with increasing K. In this case, the contribution of the non-THC flow to the mass exchange dominates that of the thermohaline flow.

When the S-S model is run in a hosing–dehosing simulation like that of the OGCM and AOGCM, the result for $K = 0$ shows the classical hysteresis loop of the Stommel model (Figure 5.6b). Much weaker hysteresis is obtained for $K = 1$, and it is shifted toward larger values of freshwater addition. As K increases upward from unity the slopes of the two stable modes approach each other and the hysteresis disappears at about $K = 2.5$. This behavior is quite similar to the transition from the hysteresis loop simulated by the uncoupled OGCM to the single curve simulated by the coupled AOGCM.

## 5.3 Assessing the Likelihood of a Human-Induced ATHC Collapse

We are now in a position to ask, 'How likely is a collapse of the Atlantic thermohaline circulation?', and if not highly unlikely, 'How can we reduce the risk of an ATHC shutdown?' To show how the significance of these questions might be investigated, and to offer some answers expressed in terms of the relative likelihood of ATHC collapse, we use the S-S model together with a simple Integrated Assessment Model, the Dynamic Integrated Climate Economy (DICE) model. DICE was developed by Bill Nordhaus (1991) to simulate a wide range of possibilities that an assessment of the more complicated process-based models cannot now exclude from the realm of possibility. More specifically, we use DICE-99 (Nordhaus and Boyer, 2001) to drive an ensemble of S-S model simulations across a range of future temperature trajectories that are themselves uncertain, given our current estimates of the range of climate sensitivity.

DICE-99 uses a reduced-form submodel (called by some the IPCC-Bern model) to calculate time-dependent GHG concentrations, radiative forcings, and change in global-mean surface air temperature from a base-case of greenhouse-gas emissions. For the latter, the climate sensitivity – the change in the equilibrium global-mean surface air temperature due to a doubling of the pre-industrial $CO_2$ concentration, $\Delta T_{2x}$ – must be prescribed. For this we use the probability density function (pdf ) calculated by Andronova and Schlesinger (2001) from the observed record of surface air temperature from 1856 to 1997, as discretized by Yohe et al. (2004). Because simple climate models have simulated an irreversible ATHC shutdown, akin to $K = 0$ in the S-S model, while our and other AOGCMs simulate a reversible ATHC shutdown akin to $K = 2.5$ in the S-S model, we take K in the S-S model to be uncertain with a uniform pdf between these values. To close the problem, we specify the (non-dimensional) amount of freshwater added to the North Atlantic, $\Pi(t)$, as a function of the change in global-mean surface air temperature simulated by DICE-99, $\Delta\bar{T}(t)$.

Results from simulations by our atmospheric GCM coupled to a 60 m deep mixed-layer ocean model for several different radiative forcings (Schlesinger et al., 2000) suggest the linear relationship,

$$\Pi(t) = \alpha[\Delta\bar{T}(t) - \Delta\bar{T}_c(t)]H\,[\Delta\bar{T}(t) - \Delta\bar{T}_c]\ ,$$

where

$$H(x) = \begin{cases} 0 \text{ if } x < 0 \\ 1 \text{ if } x \geq 0 \end{cases}$$

is the Heavyside step function and $\alpha$ is the 'hydraulic sensitivity'. The Heavyside step function is introduced to prevent any freshwater addition until a critical temperature change is reached, $\Delta\bar{T}_c$. As noted in the Appendix, we treat both $\alpha$ and $\Delta\bar{T}_c$ as uncertain independent quantities with uniform pdfs between 0.2 and 1.0 (1/°C) and between 0 and 0.6°C, respectively (Yohe et al., 2005).

The policy instrument within DICE is a tax on the carbon content of fossil fuels, from an initial tax of $10 a ton of carbon (tC) – about 5 cents a gallon of gasoline – to $100 per tC – about 6 pence per liter of petrol. This carbon tax rises through time at the then prevailing interest rate that is determined by the model. The tax can be considered as economic 'shorthand' for a wide range of possible policy interventions such as the Clean Development Mechanism and Joint Implementation.

We now address the question, 'How likely is a collapse of the Atlantic thermohaline circulation?' For the base-case $CO_2$ emission from 2005 to 2205 and $\Delta T_{2x} = 3$°C, the likelihood of an ATHC shutdown obtained over the uniform probability distributions for K, $\alpha$ and $\Delta\bar{T}_c$ rises monotonically to 4 in 10 in 2100 and 65 in 100 in 2200 (Figure 5.7(d)).

Having found that the collapse of the Atlantic thermohaline circulation is not highly unlikely, we now address the question, 'How can we reduce the risk of an ATHC shutdown?' Policy intervention in the form of a carbon tax (Figure 5.7): (1) reduces $CO_2$ emissions to zero, earlier the larger the initial tax; (2) causes the $CO_2$ concentration to peak and then decrease as the carbon sinks begin to dominate the declining $CO_2$ emissions, earlier the larger the initial tax; and (3) causes the global-mean surface temperature change to peak and then decrease in response to the declining $CO_2$ concentration, to lower values the larger the initial tax. As a result, mitigation can cause the likelihood of an ATHC shutdown to peak, with lower maximum probabilities (MP) associated with larger initial taxes.

We now consider MP as a function of the initial tax in 2005 (IT) contingent on (Figure 5.8): (a) climate sensitivity, $\Delta T_{2x}$; (b) the critical temperature threshold for the input of freshwater into the North Atlantic, $\Delta\bar{T}_c$; (c) the hydraulic sensitivity, $\alpha$; and (d) the ratio of the salt transport by the non-THC oceanic motions to that by the ATHC, K. Each of these likelihoods is obtained over the probability distributions of the three non-contingent quantities. For example, for the contingency on $\Delta T_{2x}$, the likelihood is calculated

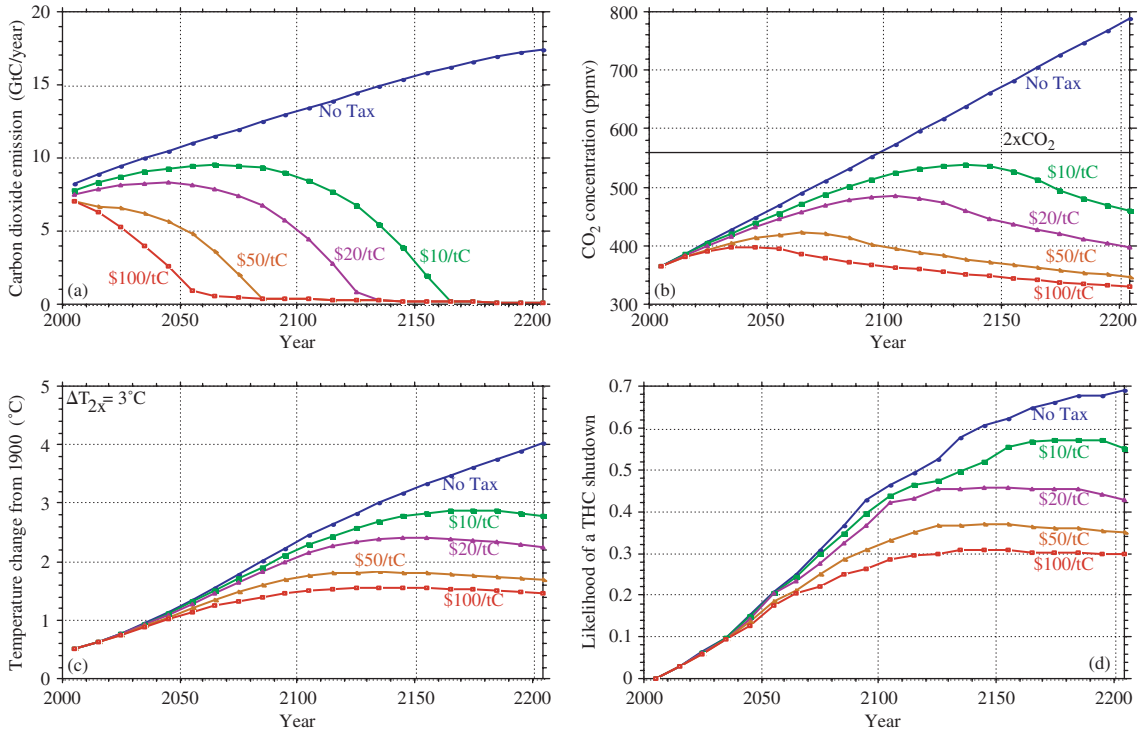


**Figure 5.7** Carbon dioxide emission (a) and atmospheric concentration (b), global-mean near-surface air temperature change (c), and the likelihood of an ATHC shutdown (d) versus time for different initial taxes.

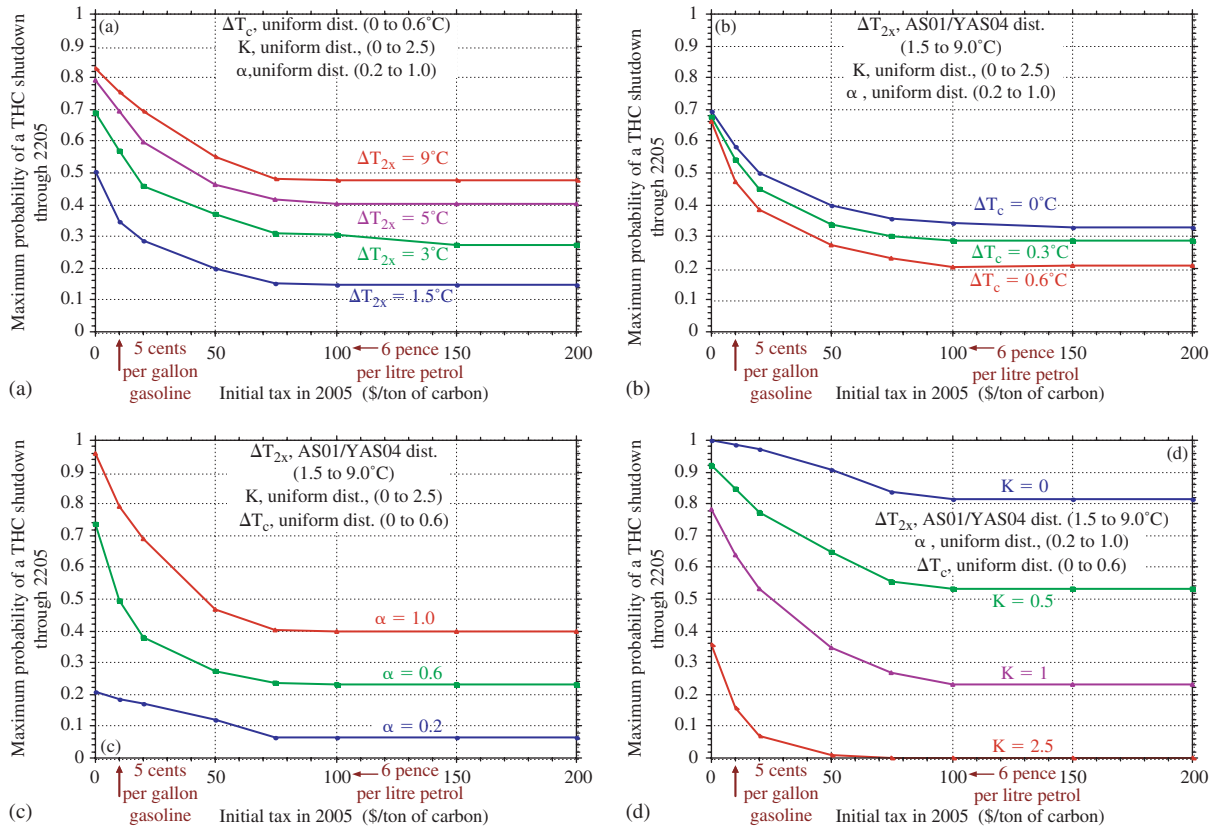


**Figure 5.8** Sensitivity of the maximum probability of an ATHC shutdown versus carbon tax to climate sensitivity, $\Delta T_{2x}$ (a); threshold temperature, $\Delta \overline{T}_c$ (b); hydraulic sensitivity $\alpha$ (c); and ratio of the non-THC transport of salinity to the ATHC transport, K (d).

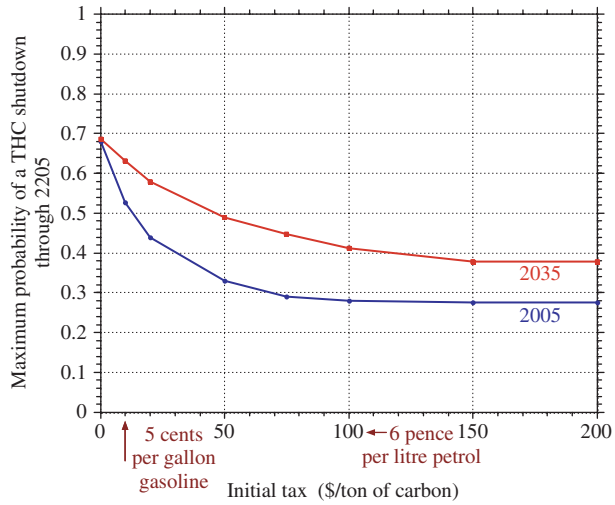


**Figure 5.9** Maximum probabilities of a collapse of the ATHC between 2005 and 2205 are plotted against various carbon taxes initiated in either 2005 or 2035. Once they are imposed, the taxes increase over time at the endogenously determined rate of interest derived by DICE-99. The probabilities were computed across a complete sample of scenarios defined by spanning all sources of uncertainty.

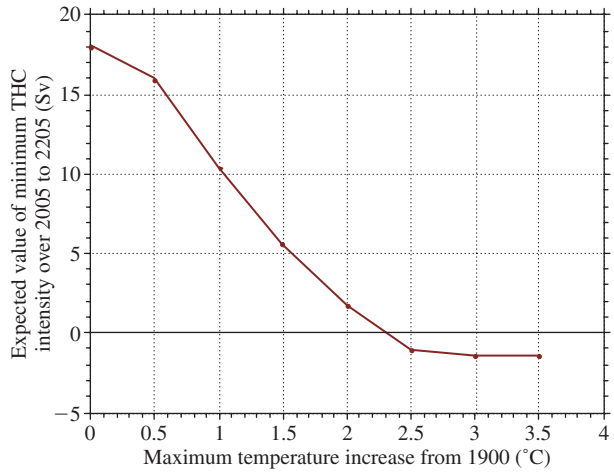


**Figure 5.10** Expected value of the minimum ATHC intensity over 2005–2205 versus global-mean temperature increase from 1990.

over the probability distributions for $\Delta\bar{T}_c$, K and $\alpha$. It is found that MP decreases with increasing IT, but the rate of decrease slows to zero when IT reaches \$100/tC. Also, the MP for any IT is most sensitive to K; that is, whether the shutdown of the ATHC is irreversible (small K) or reversible (large K). The MP–IT relationship is also sensitive to the uncertainty in hydraulic sensitivity, $\alpha$, and climate sensitivity, $\Delta T_{2x}$, but less so than to the uncertainty in K. Lastly, the MP–IT relationship is relatively insensitive to the uncertainty in the threshold, $\Delta\bar{T}_c$.

MP as a function of IT beginning in 2005 (Figure 5.9), obtained over the probability distributions of all four uncertain quantities K, $\alpha$, $\Delta T_{2x}$ and $\Delta\bar{T}_c$, is reduced from a 65-in-100 occurrence for no initial tax to a 28-in-100 occurrence for an initial tax of \$100/tC. If the tax were initiated 30 years later in 2035, then the \$100/tC tax would reduce the 65-in-100 likelihood to a 42-in-100 likelihood, and a \$200/tC tax somewhat further to a 38-in-100 occurrence. We also found the expected value of global warming required to shutdown the ATHC is 2.3°C (Figure 5.10).

## 5.4 Conclusion

We have used, of necessity, very simple models of the Earth's climate system, within DICE-99, and of the Atlantic thermohaline circulation, the S-S model. Note, though, that the latter contains the original Stommel model (for K = 0) that gave rise to the concern about the possible collapse of the ATHC. Accordingly, one should take the quantitative results with caution.

This caution notwithstanding, one cannot but be taken by the finding that in the absence of any policy intervention to slow the emission of greenhouse gases, uncertainty in our understanding of ATHC processes supports a greater than 50% likelihood of an Atlantic THC collapse. Furthermore, even with a carbon tax, this uncertainty supports a likelihood of an ATHC collapse in excess of 25%. Such high probabilities are worrisome. Of course, they should be checked by additional modelling studies. Nonetheless, simulations based on simple models do identify major sensitivities and thus provide guidance for these future studies. If further work produces similar results, it would indicate that the risk of an ATHC collapse is unacceptably large. In this case, measures over and above the policy intervention of a carbon tax should be given serious consideration.

## Acknowledgements

This material is based upon work supported by the National Science Foundation under Award No. ATM-0084270. Any opinions, findings, and conclusions or recommendations expressed in this publication are those of the authors and do not necessarily reflect the views of the National Science Foundation. The authors express their gratitude to Tom Wigley and two anonymous referees for constructive comments on the earlier draft of this paper. GY also acknowledges the support of B. Belle. Remaining errors, of course, reside with the authors.

## APPENDIX

### Calibration of the Stommel-Saltzman Model

The governing equation of the Stommel-Saltzman (S-S) 2-box ocean model for nondimensional variables is

$$\frac{ds}{dt^*} = \Pi - |1 - s|s - Ks, \tag{5.1}$$

where s is the difference in salinity between the equatorial and polar boxes, t* is time, $\Pi$ is the freshwater addition, and K is the ratio of the transport coefficient for the gyre circulation and eddies (denoted $k_\phi$) to that for the ATHC (denoted $k_\psi$). The K term was absent from the original Stommel model and was taken to be as large as unity by Saltzman. The maximum streamfunction of the ATHC is

$$\Psi = k_\psi \mu_T \delta T^*(1 - s), \tag{5.2}$$

where $\mu_T$ is the thermal volume expansion coefficient, and $\delta T^*$ is the temperature difference between the equatorial and polar boxes, taken to be constant.

We calibrated the S-S model so that it is about as sensitive to a freshwater addition as the University of Illinois at Urbana-Champaign (UIUC) coupled atmosphere-ocean general circulation model (AOGCM), which requires a freshwater addition of 0.6 Sv ($10^6$ $m^3$/sec) between 50°N to 70°N in the Atlantic to shut down the ATHC [Yin (2004); Yin et al. (2005)]. From Equation (5.2), an ATHC shutdown ($\Psi = 0$) requires $s = 1$. From the steady-state version of Equation (5.1), the latter condition requires a dimensionless freshwater addition of $\Pi = K$. The corresponding dimensional freshwater addition is $F = \beta\Pi = \beta K$, where $\beta$ is a conversion coefficient. The largest value of K we consider is $K = 2.5$, which is the value required by the S-S model to reproduce the reversible ATHC shutdown simulated by the UIUC AOGCM [Yin (2004); Yin et al. (2005)]. Taking $F = 0.6$ Sv for $K = 2.5$ yields $\beta = 0.24$ Sv.

Schlesinger et al. (2000) report results from simulations by the UIUC atmospheric GCM coupled to a 60 m deep mixed-layer ocean model for several different radiative forcings that suggest a linear relationship between freshwater addition, $\Pi$, and global-mean temperature change, $\Delta\bar{T}$,

$$\Pi(t) = \alpha[\Delta\bar{T}(t) - \Delta\bar{T}_c]H[\Delta\bar{T}(t) - \Delta\bar{T}_c], \tag{5.3}$$

where

$$H(x) = \begin{cases} 0 \text{ if } x < 0 \\ 1 \text{ if } x \geq 0 \end{cases} \tag{5.4}$$

is the Heavyside step function and $\alpha$ is the 'hydraulic sensitivity'. The Heavyside step function is introduced to prevent any freshwater addition until a critical temperature change, $\Delta\bar{T}_c$, is reached.

Substituting Equation. (5.3) into $F = \beta\Pi$ and solving for $\alpha$ yields

$$\alpha = \frac{F}{\beta[\Delta\bar{T} - \Delta\bar{T}_c]H[\Delta\bar{T} - \Delta\bar{T}_c]} \tag{5.5}$$

If we assume that $\Delta\bar{T} - \Delta\bar{T}_c = 2.5$°C for $F = 0.6$ Sv, then $\alpha = 1.0\ (°C)^{-1}$ for $\beta = 0.24$ Sv. The values of $\alpha$ and $\Delta\bar{T}_c$ are highly uncertain, though. Accordingly, we took these quantities to have uniform probability distributions between 0.2 and 1.0 $(°C)^{-1}$ (in increments of 0.2) for $\alpha$ and between 0.0°C and 0.6°C (in 0.1 degree increments) for $\Delta\bar{T}_c$.

Finally, the S-S model translates freshwater addition to flow in the ATHC. Yin (2004) and Yin et al. (2005) show that this depends critically on the ratio of salinity transports by the gyre/eddies and the ATHC, represented by K. A uniform prior ranging from 0.0 through 2.5 (in six increments of 0.5) was chosen based on the study by Yin (2004) and Yin et al. (2005) which showed that the S-S model with $K = 0$ (the original Stommel model) reproduced the irreversible ATHC shutdown simulated by the uncoupled UIUC ocean general circulation model, while the S-S model with $K = 2.5$ reproduced the reversible ATHC shutdown simulated by the coupled UIUC atmosphere-ocean general circulation model.

The likelihood of any specific combination of climate sensitivity, $\Delta\bar{T}_c$, $\alpha$, and K thus equaled ($\pi_i$/210), where $\pi_i$ represents the likelihood of the various climate sensitivities.

## REFERENCES


Alley, R.B. (1998) Palaeoclimatology: Icing the North Atlantic. *Nature,* **392**, 335–337.

Alley, R.B. (2000) The Younger Dryas cold interval as viewed from central Greenland. *Quaternary Sci. Rev.,* **19**, 213–226.

Alley, R.B., Meese, D.A., Shuman, C.A., Gow, A.J., Taylor, K.C., Grootes, P.M., White, J.W.C., Ram, M., Waddington, E.D., Mayewski, P.A. and Zielinski, G.A. (1993) Abrupt increase in Greenland snow accumulation at the end of the Younger Dryas event. *Nature,* **362**, 527–529.

Andronova, N.G. and Schlesinger, M.E. (2001) Objective estimation of the probability density function for climate sensitivity. *J. Geophys. Res.,* **106**, 22, 605–22, 612.

Atkinson, T.C., Briffa, K.R. and Coope, G.R. (1987) Seasonal temperatures in Britain during the past 22,000 years, reconstructed using beetle remains. *Nature,* **325**, 587–592.

Broecker, W.S. (1985) Does the ocean-atmosphere system have more than one stable mode of operation? *Nature,* **315**, 21–26.

Broecker, W.S. (1997) Thermohaline Circulation, the Achilles Heel of Our Climate System: Will Man-Made $CO_2$ Upset the Current Balance? *Science*, **278**, 1582–1588.

Broecker, W.S. (2003) Does the Trigger for Abrupt Climate Change Reside in the Ocean or in the Atmosphere? *Science,* **300**, 1519–1522.

Broecker, W.S., Andree, M., Wolfi, W., Oeschger, H., Bonani, G., Kennett, J. and Peteet, D. (1988) The chronology of the last deglaciation: Implications to the cause of the Younger Dryas event. *Paleoceanography,* **3**, 1–19.

Broecker, W.S., Kennett, J.P., Flower, B.P., Teller, J., Trumbore, S., Bonani, G. and Wolfi, W. (1989) The routing of Laurentide ice-sheet meltwater during the Younger Dryas cold event. *Nature,* **341**, 318–321.

Chinzei, K., Fujioka, K., Kitazato, H., Koizumi, I., Oba, T., Oda, M., Okada, H., Sakai, T. and Tanimura, Y. (1987) Postglacial environmental change of the Pacific Ocean off the coasts of central Japan. *Marine Micropaleontology,* **11**, 273–291.

Crichton, M. (2004) *State of Fear,* New York, HarperCollins, pp. 603.

Cubasch, U., *et al.* 2001: Projections of future climate change. In: *Climate Change 2001: The Scientific Basis. Contribution of Working Group I to the Third Assessment Report of the Intergovernmental Panel on Climate Change* [Houghton, J.T., et al., Eds.]. Cambridge University Press, Cambridge, UK, pp. 525–582.

Emmerich, R. (2004) The Day After Tomorrow. 20th Century Fox, http://www.foxhome.com/dayaftertomorrow/

Gagosian, R.B. (2003) Abrupt Climate Change: Should We Be Worried? Woods Hole, MA, Woods Hole Oceanographic Institution, http://www.whoi.edu/institutes/occi/currenttopics/climatechange_wef.html

Ganopolski, A. and Rahmstorf, S. (2001) Rapid changes of glacial climate simulated in a coupled climate model. *Nature,* **409**, 153–158.

Johnson, R.G. and McClue, B.T. (1976) A model for northern hemisphere continental ice sheet variation. *Quaternary Research,* **6**, 325–353.

Leggett, J., Pepper, W.J. and Swart, R.J., 1992: Emissions scenarios for the IPCC: An update. (In) *Climate Change 1992: The Supplementary Report to the IPCC Scientific Assessment* [Houghton, J.T., et al., Eds.]. Cambridge University Press, Cambridge, UK, pp. 71–95.

Lempert, R.J. and Schlesinger, M.E. (2000) Robust Strategies for Abating Climate Change. *Climatic Change,* **45**, 387–401.

Manabe, S. and Stouffer, R.J. (1994) Multiple-century response of a coupled ocean-atmosphere model to an increase of atmospheric carbon dioxide. *J. Climate,* **7**, 5–23.

Manabe, S. and Stouffer, R.J. (1988) Two Stable Equilibria of a Coupled Ocean-Atmosphere Model. *J. Climate,* **1**, 841–866.

Manabe, S. and Stouffer, R.J. (1999) Are two modes of thermohaline circulation stable? *Tellus,* **51A**, 400–411.

McManus, J.F. (2004) Palaeoclimate: A great grand-daddy of ice cores. *Nature,* **429**, 611–612.

McManus, J.F., Francois, R., Gherardi, J.-M., Keigwin, L.D. and Brown-Leger, S. (2004) Collapse and rapid resumption of Atlantic meridional circulation linked to deglacial climate change. *Nature,* **428**, 834–837.

Nesje, A., Dahl, S.O. and Bakke, J. (2004) Were abrupt late glacial and early-Holocene climatic changes in northwest Europe linked to freshwater outbursts to the North Atlantic and Arctic Oceans? *The Holocene,* **14**, 299–310.

Nordhaus, W.D. (1991) To slow or not to slow? *Economic Journal,* **5**, 920–937.

Nordhaus, W.D. and Boyer, J. (2001) *Warming the World – Economic Models of Global Warming,* MIT Press, Cambridge, MA.

Prange, M., Romanova, V. and Lohmann, G. (2002) Influence of vertical mixing on the thermohaline hysteresis: analyses of an OGCM. *J. Phys. Oceanogr.,* **33**, 1707–1721.

Rahmstorf, S. (1995) Bifurcations of the Atlantic thermohaline circulation in response to changes in the hydrological cycle. *Nature,* **378**, 145–149.

Rind, D., Demenocal, P., Russell, G., Sheth, S., Collins, D., Schmidt, G. and Teller, J. (2001) Effects of glacial meltwater in the GISS coupled atmosphere-ocean model. *J. Geophys. Res.,* **106**, 27, 335–27, 353.

Robinson, K.S. (2004) *Forty Signs of Rain,* New York, Bantam Dell, pp. 358.

Rooth, C. (1982) Hydrology and ocean circulation. *Prog. Oceanogr.,* **11**, 131–139.

Saltzman, B. (2002) *Dynamical Paleoclimatology: Generalized Theory of Global Climate Change,* San Diego, Academic Press.

Schiller, A., Mikolajewicz, U. and Voss, R. (1997) The stability of the North Atlantic thermohaline circulation in a coupled ocean-atmosphere general circulation model. *Climate Dynamics,* **13**, 325–347.

Schlesinger, M.E., Malyshev, S., Rozanov, E.V., Yang, F., Andronova, N.G., Vries, B.D., Grübler, A., Jiang, K., Masui, T., Morita, T., Penner, J., Pepper, W., Sankovski, A. and Zhang, Y. (2000) Geographical Distributions of Temperature Change for Scenarios of Greenhouse Gas and Sulfur Dioxide Emissions. *Technological Forecasting and Social Change,* **65**, 167–193.

Schmittner, A. and Weaver, A.J. (2001) Dependence of multiple climate states on ocean mixing parameters. *Geophys. Res. Lett.,* **28**, 1027–1030.

Schmittner, A., Yoshimori, M. and Weaver, A.J. (2002) Instability of glacial climate in a model of ocean-atmosphere-cryosphere system. *Science,* **295**, 1489–1493.

Schwartz, P. and Randall, D. (2003) An abrupt climate change scenario and its implications for United States national security, http://pubs.acs.org/cen/topstory/8209/pdf/climatechange.pdf

Stommel, H.M. (1961) Thermohaline convection with two stable regimes of flow. *Tellus,* **13**, 224–230.

Tarasov, L. and Peltier, W.R. (2005) Arctic freshwater forcing of the Younger Dryas cold reversal. *Nature,* **435,** 662–665.

Taylor, K.C., Mayewski, P.A., Alley, R.B., Brook, E.J., Gow, A.J., Grootes, P.M., Meese, D.A., Saltzman, E.S., Severinghaus, J.P., Twickler, M.S., White, J.W.C., Whitlow, S. and Zielinski, G. (1997) The Holocene-Younger Dryas Transition Recorded at Summit, Greenland. *Science,* **278**, 825–827.

Teller, J.T., Leverington, D.W. and Mann, J.D. (2002) Freshwater outbursts to the oceans from glacial Lake Agassiz and their role in climate change during the last deglaciation. *Quaternary Science Reviews,* **21**, 879–887.

Titz, S., Kuhlbrodt, T., Rahmstorf, S. and Feudel, U. (2002) On freshwater-dependent bifurcation in box model of the interhemispheric thermohaline circulation. *Tellus,* **54A**, 89–98.

Vellinga, M., Wood, R.A. and Gregory, J.M. (2002) Processes governing the recovery of a perturbed thermohaline circulation in HadCM3. *J. Climate,* **15**, 764–780.

Yin, J. (2004) The Reversibility/Irreversibility of the Thermohaline Circulation after its Shutdown: Simulations from a Hierarchy of Climate Models. *Atmospheric Sciences.* Urbana, University of Illinois at Urbana-Champaign.

Yin, J., Schlesinger, M.E., Andronova, N.G., Malyshev, S. and Li, B. (2005) Is a Shutdown of the Thermohaline Circulation Irreversible? *J. Geophys. Res.,* (submitted).

Yohe, G., Andronova, N. and Schlesinger, M. (2004) To Hedge or Not Against an Uncertain Climate Future. *Science,* **306**, 416–417.

Yohe, G., Schlesinger, M.E. and Andronova, N.G. (2005) Reducing the Risk of a Collapse of the Atlantic Thermohaline Circulation. *Integrated Assessment,* (submitted).